Viscosity of confined two-dimensional Yukawa liquids: A nonequilibrium method

S. Landmann, H. Kählert, H. Thomsen, and M. Bonitz

Citation: Physics of Plasmas **22**, 093703 (2015); doi: 10.1063/1.4930546
View online: http://dx.doi.org/10.1063/1.4930546
View Table of Contents: http://scitation.aip.org/content/aip/journal/pop/22/9?ver=pdfcov
Published by the AIP Publishing

Viscosity of confined two-dimensional Yukawa liquids: A nonequilibrium method

S. Landmann,[1] H. Kählert,[2] H. Thomsen,[2] and M. Bonitz[2]
[1]Universität Leipzig, Institut für Theoretische Physik, Brüderstr. 16, 04103 Leipzig, Germany
[2]Christian-Albrechts-Universität zu Kiel, Institut für Theoretische Physik und Astrophysik, Leibnizstr. 15, 24098 Kiel, Germany

(Received 24 July 2015; accepted 27 August 2015; published online 11 September 2015)

We present a nonequilibrium method that allows one to determine the viscosity of two-dimensional dust clusters in an isotropic confinement. By applying a tangential external force to the outer parts of the cluster (e.g., with lasers), a sheared velocity profile is created. The decay of the angular velocity towards the center of the confinement potential is determined by a balance between internal (viscosity) and external friction (neutral gas damping). The viscosity can then be calculated from a fit of the measured velocity profile to a solution of the Navier-Stokes equation. Langevin dynamics simulations are used to demonstrate the feasibility of the method. We find good agreement of the measured viscosity with previous results for macroscopic Yukawa plasmas. © *2015 AIP Publishing LLC*. [http://dx.doi.org/10.1063/1.4930546]

I. INTRODUCTION

Dusty plasmas contain, in addition to the usual plasma components (electrons, ions, and neutral particles), small dust particles with a size on the order of a few micrometers.[1] Negatively charged by the influx of electrons on their surface, the dust particles interact with each other through electrostatic forces that are screened by the plasma environment.[2] For typical experimental parameters, the charges on the dust particles are on the order of a few thousand. As a result, the interactions become dominant, and the dust subsystem can be considered a strongly coupled plasma. Dusty plasmas can form ordered structures such as dust lattices,[3] and shell[4] or ring structures,[5] depending on the experimental geometry. In addition to their ability to crystallize, also the liquid state is of high interest since many liquid properties can be investigated by studying the movement of individual particles. This includes diffusion processes,[6] heat transport,[7] or wave propagation.[8]

We concentrate here on two-dimensional systems, where the particles are located at the same height above the lower electrode in a rf discharge and form a layer, i.e., the vertical confinement is much stronger than the horizontal confinement. The interactions between the dust particles can then be modeled by a simple Yukawa potential

$$\phi(r) = \frac{Q^2}{r} e^{-r/\lambda}, \tag{1}$$

where λ is the (effective) screening length, Q the particle charge, and r their horizontal separation. The out-of-plane interactions between particles at different heights can be significantly modified by ion flows towards the lower electrode, which lead to oscillatory dust potentials in the streaming direction. However, the in-plane interactions are well described by the Yukawa potential with an effective screening length that is determined by the plasma parameters (ion flow speed, ion-neutral damping, etc.).[9] Since it can describe a variety of different situations, the Yukawa potential is not only widely used to study the properties of two-dimensional dust ensembles but also highly relevant for colloidal systems.[10]

The transport properties of two- and three-dimensional *Yukawa liquids*[11,12] such as diffusion,[6,13] heat conductivity,[14,15] or viscosity[16–25] are accessible via molecular dynamics (MD) simulations and often allow for a direct comparison with experiments. The Green-Kubo relations can be exploited to calculate the viscosity η with equilibrium MD simulations. In contrast, nonequilibrium MD simulations often impose certain velocity profiles to determine η, see Ref. 26 for an overview. Experimentally, laser beams can be used to create a sheared flow of dust particles, which carries information about the viscosity.[22,27–30]

In this work, we use a nonequilibrium method to determine the viscosity of isotropically confined two-dimensional dust clusters, extending previous simulations for the heat transport.[14] The method requires an external force to manipulate the dust particles, which can be realized experimentally with lasers, as was already demonstrated.[31–34] The force is directed in the tangential direction and sets the outer part of the cluster into rotation. Due to the interaction between the particles, some of the angular momentum is transported to the inner part of the cluster, which therefore also starts to rotate. However, at the same time, friction with the neutral gas removes angular momentum. The result is a stationary nonequilibrium state with a tangential velocity profile that is determined by a balance between internal and external friction. The viscosity can be inferred from a fit of experimental or, in the present case, simulation data for the velocity profile to an analytical solution of the Navier-Stokes equation, similar to previous work.[22,27,29] We compare our Langevin dynamics simulation results for confined Yukawa systems with simulations for extended 2D Yukawa plasmas[19,20] and find good agreement.

This paper is organized as follows. In Sec. II, we present the details of our MD simulation method and the analytical solution of the Navier-Stokes equation. The viscosity is

calculated from a fit of the simulation data to the theoretical velocity profile in Sec. III. The results are compared with previous simulation data for 2D Yukawa plasmas. Limitations of the model are discussed in Sec. IV. We conclude with a summary of the results in Sec. V.

II. METHODS

Our method for determining the viscosity is based on fitting the results of MD simulations to a solution of the Navier-Stokes equations. In the following, we first describe the simulation technique and, in a second step, a practical way of obtaining a fit function from the Navier-Stokes equations.

A. Molecular dynamics simulations

The simulations are performed for a medium-size cluster with $N = 149$ particles. As was mentioned in the Introduction, the particles interact via the Yukawa potential, Eq. (1). The confinement potential is modeled as an isotropic harmonic trap, $V(r) = m\omega_0^2 r^2/2$, where ω_0 is the trap frequency and m the dust particle mass. This model was successfully applied to describe the structure and dynamics of dust clusters in experiments, e.g., Refs. 34 and 35. Neutral gas damping is accounted for by including a friction and a random force in the equation of motion (Langevin dynamics)

$$m\dot{\boldsymbol{v}}_i = -\nabla_i V(\boldsymbol{r}_i) - \nabla_i \sum_{j\neq i} \phi(|\boldsymbol{r}_i - \boldsymbol{r}_j|) - m\nu\boldsymbol{v}_i + \boldsymbol{f}_i + \boldsymbol{F}_L, \tag{2}$$

where ν is the friction coefficient, $\boldsymbol{f}_i$ the random force with $\langle f_i^\alpha(t) f_j^\beta(t')\rangle = 2m\nu k_B T \delta_{ij}\delta^{\alpha\beta}\delta(t-t')$ $(\alpha, \beta = x, y)$, and $\boldsymbol{F}_L$ an external driving force. The temperature of the neutral gas is denoted by T. For the integration of the system, we use the Symplectic Low-Order scheme by Mannella.[36] The friction coefficient is chosen to be $\nu = 1.1\,\omega_0$ throughout all simulations, corresponding to intermediate damping.

The simulations are performed in the following way. After an initial equilibration phase without external driving force, at $\omega_0 t = 30$, a Gaussian-shaped force

$$\boldsymbol{F}_L(\boldsymbol{r}) = A\,\frac{Q^2/r_0}{\sigma\sqrt{2\pi}}\exp[-(r-R_L)^2/2\sigma^2]\mathbf{e}_\phi, \tag{3}$$

centered at $r = R_L$, with (dimensionless) amplitude A and variance σ, acts on the outer part of the cluster. We have also introduced the characteristic length scale $r_0 = (2Q^2/m\omega_0^2)^{1/3}$. The force is directed in the tangential direction and forces the outer part of the cluster to perform a rotation. Angular momentum is also transferred to the inner parts of the cluster, and a stationary velocity profile develops. The measurement of the angular velocity profile begins at $\omega_0 t = 36$. Figure 1 depicts a cluster in the stationary case for a screening parameter $r_0/\lambda = 3$ and a temperature $\tilde{T} = T/T_0 = 0.04$, where $T_0 = Q^2/(r_0\, k_B)$.

B. Analytical model

To extract the viscosity from the velocity profile, we compare the simulation results with the solution of the Navier-Stokes equations for our system. We obtain an analytical fit function, where the ratio of the external (neutral gas) and internal friction (viscosity) determines the decrease of the tangential velocity from the boundary towards the center of the cluster, see Refs. 22 and 27 for a closely related method with a different geometry. The viscosity can be determined from a fit to the simulation data.

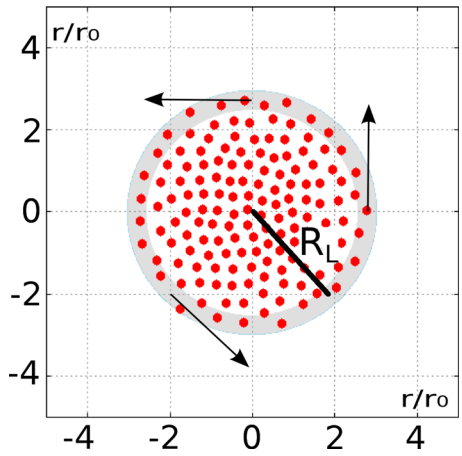

FIG. 1. A cluster of 149 particles for $r_0/\lambda = 3$ and $\tilde{T} = 0.04$. The gray area illustrates the region in which the tangential force acts. The arrows exemplify the direction of the force.

The momentum equation for the dust fluid [described by a density profile $n(\boldsymbol{r}, t)$ and velocity field $\boldsymbol{v}(\boldsymbol{r}, t)$] is given by[27]

$$mn\left[\frac{\partial \boldsymbol{v}}{\partial t} + (\boldsymbol{v}\cdot\nabla)\boldsymbol{v}\right] = -\nabla p - nq\nabla\Phi - n\nabla V + \eta\Delta\boldsymbol{v} - m\nu n\boldsymbol{v} + n\boldsymbol{F}_L. \tag{4}$$

Here, p denotes the pressure, Φ the electrostatic potential, and η the shear viscosity. We only require the stationary limit of Eq. (4) with $\partial\boldsymbol{v}/\partial t = 0$, which describes the fluid after the relaxation phase, i.e., in the limit $t \to \infty$. Due to the symmetry of the trapping potential and the tangential driving force, the resulting velocity profile is of the form $\boldsymbol{v}(\boldsymbol{r}) = v_\phi(r)\,\hat{\boldsymbol{e}}_\phi$, where $\hat{\boldsymbol{e}}_\phi$ is the unit vector in the tangential direction. This implies $\nabla\cdot\boldsymbol{v} = 0$, which has already been accounted for in Eq. (4).

We can now separate Eq. (4) into the radial and tangential components, which yields two coupled equations for the density profile $n(r)$ and the tangential velocity. While it would, in principle, be possible to solve these equations self-consistently with a given equation of state for the pressure, Poisson's equation for the potential, and the viscosity as a free parameter, we chose a different method.

The tangential equation follows from Eq. (4) as

$$\left(\frac{\partial^2 v_\phi}{\partial r^2} + \frac{1}{r}\frac{\partial v_\phi}{\partial r} - \frac{v_\phi}{r^2}\right)\eta - m\nu n v_\phi = 0. \tag{5}$$

We have thereby exploited the symmetry of the problem, namely, that the pressure, electrostatic potential, and the confinement potential have only a radial dependence, and, hence, give no contribution. The laser driving force will be replaced by a suitable boundary condition at $r = R$, $v_\phi(R) = v_R$. A very simple way to obtain an analytical

solution for $v_\phi(r)$ is to approximate the inhomogeneous cluster with a constant density, i.e., we neglect the radial equation for $n(r)$ and use the assumption $n(r) = n_0 = \text{const.}$ to solve Eq. (5) for $v_\phi(r)$. Although this procedure is not fully consistent, it yields a surprisingly accurate fit for the velocity profile measured in the simulation, see Sec. III.

The solution of Eq. (5) for a constant density and the boundary conditions $v_\phi(R) = v_R$ and $v_\phi(0) = 0$ is given by

$$v_\phi(r) = v_R \frac{I_1\left(\sqrt{\frac{m\nu n_0}{\eta}}r\right)}{I_1\left(\sqrt{\frac{m\nu n_0}{\eta}}R\right)}, \quad r < R, \tag{6}$$

where $I_1(z)$ is a modified Bessel function of the first kind.[37] The parameters of this function are known (input parameters) or can be measured in the simulation, except for η. This makes it possible to use Eq. (6) as a fit function for the determination of the viscosity. We use the velocity v_R at $r = R$ as a fit parameter to allow the fit to match best with the simulation data. The average particle density is estimated as $n_0 = N/(\pi R_c^2)$, where R_c is the radius of the cluster. The radius is determined as the distance from the center at which the particle density drops to 5% of its maximum value. In general, we then have $R_L \neq R_c \neq R$.

In experiments, a precise determination of the friction coefficient ν is important because the fit only yields the ratio ν/η. The friction coefficient can be estimated with the Epstein formula[38] based on the neutral gas pressure, see also Ref. 27. A more direct measurement is possible, e.g., with a phase-resolved resonance method,[39] which could be used to predetermine ν for a single dust grain. It yields results that are in good agreement with the Epstein relation.[40] If the size distribution of the dust particles is sufficiently narrow, the obtained damping constant could also be employed for the experiment with many particles.

III. DETERMINATION OF VISCOSITY

We will now present the results from the MD simulations and use the measured velocity profile to calculate the viscosity coefficient.

A. Velocity, density, and temperature profiles

Figure 2 shows typical simulation results for $r_0/\lambda = 3$ and different temperatures. Also shown is the tangential driving force. The density profile shows a shell structure for the outer parts of the cluster.[41,42] The angular velocity, $\omega(r) = v_\phi(r)/r$, attains its maximum where the force is maximal and decreases in the direction of the cluster center. For the lowest temperature, $\tilde{T} = 0.04$, the influence of the shell structure on the angular velocity profile becomes apparent. Similar to the density profile, it also exhibits some minor modulations. The noisy part of the velocity profile for $r/r_0 > 3$ is caused by particles leaving the cluster for short times during which they can attain high velocities. As only the inner part of the cluster is relevant for the calculations, this does not pose a problem.

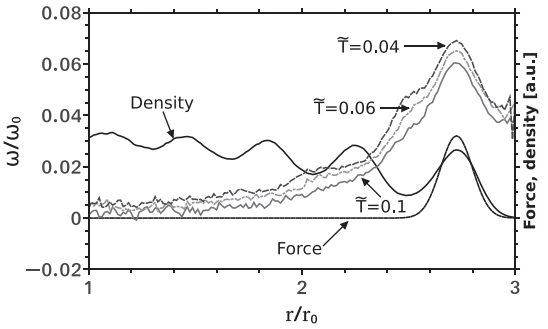

FIG. 2. Angular velocity profile $\omega(r)$ of a cluster with a screening parameter $r_0/\lambda = 3$ and various temperatures (as indicated by the arrows). The particle density is shown for the case $\tilde{T} = 0.06$. The dotted line represents the tangential force.

Since strong shear flows can lead to shear heating in regions with high velocity gradients,[43] which may affect our results, we investigated the radial temperature profile $T(r)$ of the cluster. The temperature profile was determined by measuring the average variance of the velocity of the dust particles in dependence of the radial distance from the center of the cluster. Figure 3 shows the temperature profile for three different neutral gas temperatures and a screening parameter $r_0/\lambda = 2$ for the stationary, rotating case. We observe constant temperatures for $\tilde{T} = 0.7$ and $\tilde{T} = 0.1$, even in the region with maximum shear (vertical dotted line). At $\tilde{T} = 0.04$, the radially resolved temperature deviates only slightly from the neutral gas temperature close to the location of maximum shear. Thus, for the chosen simulation parameters, we observe no significant shear heating.

B. Fitting the data

Figure 4 shows a fit of Eq. (6) for three different temperatures and a screening parameter $r_0/\lambda = 2$. The section close to the origin is omitted because the numerical data are very noisy. The good agreement of the fits with the numerically obtained velocity profiles shows that the analytical model is a good approximation for the system. The fit for $\tilde{T} = 0.2$ [Fig. 4(b)] matches the numerical data best. The deviations for $\tilde{T} = 0.04$ are caused by the inhomogeneous density

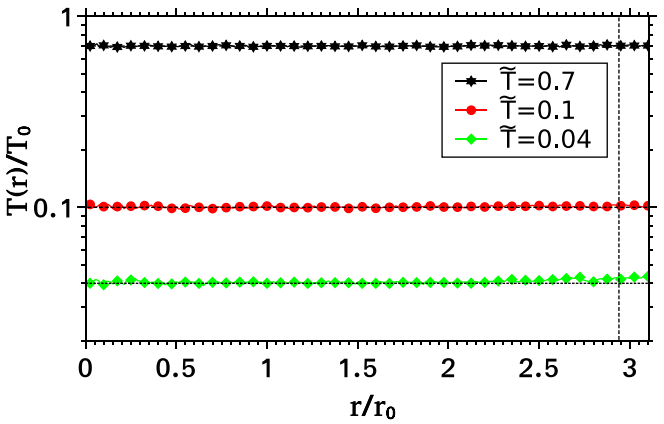

FIG. 3. Temperature profile $T(r)/T_0$ for $r_0/\lambda = 2$ and three different neutral gas temperatures $\tilde{T}$. The vertical dotted line marks the region of maximum shear.

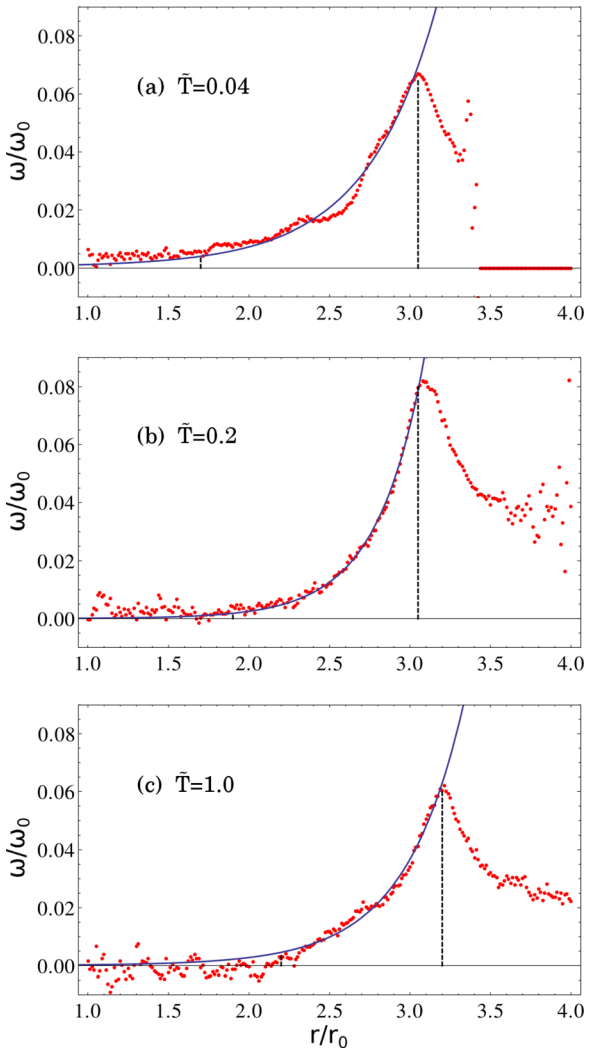

FIG. 4. Comparison of the numerical results and the fit for the angular velocity profile for a screening parameter $r_0/\lambda = 2$. The points (red) show the data from the simulations, the line (blue) is the corresponding fit. The black dotted lines mark the area that was used for the fit.

profile, which shows a shell structure at this temperature. A local maximum of the density causes the mismatch from $r/r_0 = 2.4$ to $r/r_0 = 2.7$. A comparison of the density and angular velocity of Fig. 2 for $\tilde{T} = 0.04$ shows the same effect.

The cluster expands as the temperature is increased. To make sure that only the outer part of the cluster lies in the range of the external force, it is necessary to shift the center of the force further away from the center. This also shifts the maximum of the velocity profile as can be seen by comparison of the graphs for $\tilde{T} = 0.04$ and $\tilde{T} = 1$ in Fig. 4. We further observe a decrease of the maximum of the velocity profile if the external force is kept constant. As a consequence, the data get too noisy to be evaluated properly for high temperatures, which makes it necessary to increase the amplitude of the force. In our simulations, we use a range $A = 0.45\ldots0.75$ from low to high temperatures. For the estimation of a realistic error, it is most practicable to fit the data for several slightly modified ranges and average densities and use the maximum and minimum value as error range.

C. Comparison with results for macroscopic 2D Yukawa plasmas

A macroscopic two-dimensional Yukawa plasma with (areal) density n and temperature T is fully characterized by the coupling parameter Γ and the screening parameter κ, defined by[44]

$$\Gamma = \frac{Q^2}{a\, k_B T}, \quad \kappa = \frac{a}{\lambda}. \tag{7}$$

The Wigner-Seitz radius a follows from the relation $n\pi a^2 = 1$. To compare our results for the cluster with those for a macroscopic system, we identify the average trap density $n_0 = N/(\pi R_c^2)$ with the density n of the macroscopic system. The transformation rules then become

$$\Gamma = \frac{\sqrt{n_0 r_0^2\,\pi}}{\tilde{T}}, \quad \kappa = \frac{r_0/\lambda}{\sqrt{n_0 r_0^2\,\pi}}. \tag{8}$$

The viscosity will be given in units of $\eta_0 = m n_0 \omega_p a^2$, where $\omega_p = [2Q^2/(ma^3)]^{1/2}$, see Ref. 20. We compare our results to equilibrium[19] and nonequilibrium[20] molecular dynamics simulation. For a fixed value of r_0/λ, the temperature $\tilde{T}$ is varied to study the viscosity as a function of the coupling parameter Γ. Since the average particle density is temperature dependent, κ also varies slightly, see Eq. (8). This makes it somewhat difficult to compare the results for a wide temperature range since the variations in κ become too large.

Figure 5 shows the results from the equilibrium molecular dynamics simulations of Ref. 19 for $\kappa = 0.56$ and the results from our simulation[45] for $\kappa \approx 0.54\ldots0.65$. We find good agreement, especially for the position of the minimum of the viscosity. As can be seen from the screening parameters given in Fig. 5, κ deviates from the desired value of $\kappa = 0.56$ as Γ approaches low or high values, which is due to variations of the average density. In addition, the simulations of Ref. 19 have been performed with a Nosé-Hoover thermostat while we use Langevin dynamics that includes friction with the neutral gas, see Refs. 46–49. In 3D Yukawa liquids, friction was shown to decrease (increase) the viscosity for low (high) coupling.[47] Figure 6 displays the viscosity obtained from nonequilibrium molecular dynamics simulations[20] for $\kappa = 1$

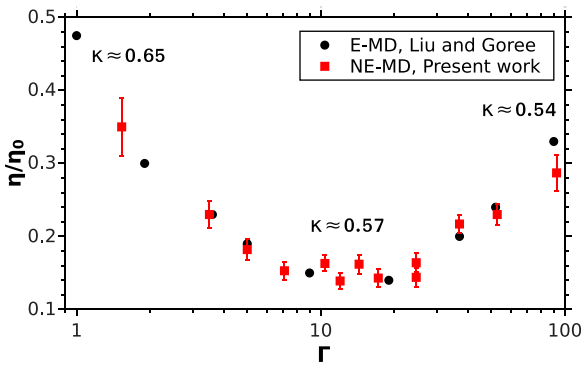

FIG. 5. Comparison of the equilibrium MD simulations of Ref. 19 for $\kappa = 0.56$ (black dots) with our simulations results (red squares, $r_0/\lambda = 2$). The variation of the screening parameter κ in our simulations can be inferred from the numbers given in the figure.

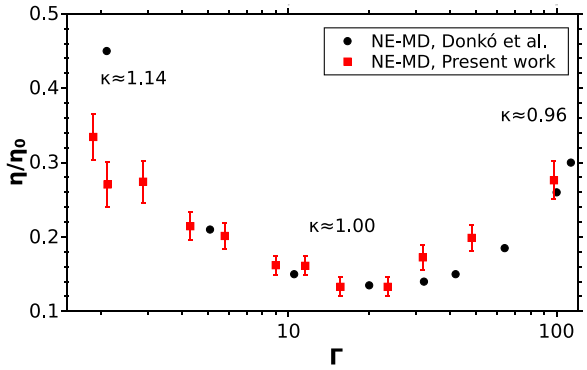

FIG. 6. Comparison of the nonequilibrium MD simulations of Ref. 20 for $\kappa = 1$ (black dots) with our simulations results (red squares, $r_0/\lambda = 4.7$). The variation of the screening parameter κ in our simulations can be inferred from the numbers given in the figure.

(method 1 in Ref. 20 with $N = 3960$ particles) and the results from our simulation for $\kappa \approx 0.96\ldots1.14$. Again, we find fair agreement between the two methods, in particular, the locations of the minima differ only slightly. As in the previous case, the deviations increase for very high or very low Γ.

To summarize, the general agreement of our results with those for a macroscopic Yukawa plasma is surprisingly good, given the small size of the cluster and the fact that the trapped cluster is, in many aspects, different from a uniform plasma. This includes the existence of an outer boundary, the inhomogeneous density profile, and the confinement potential.

IV. DISCUSSION

In this section, we discuss some of the limitations of the model.

A natural restriction is that the dust cluster must be in the liquid state. This excludes very high coupling strengths where the particles would eventually crystallize. In this case, a weak force was found to lead to a rigid rotation of the cluster whereas an isolated rotation of the outer shell is observed for a strong force. While there are no phase transition in a small cluster in the thermodynamic sense, it is possible to identify temperature ranges where the cluster shows properties of a liquid or more closely resembles a solid.[50] Another restriction arises from the density profile, which shows strong modulations at high coupling. These shell structures also appear in the radial velocity profile and restrict the use of Eq. (6) as a fit function, since the shell structure is not included in the analytical model. An accurate theoretical description of the density profile for confined Yukawa systems must include correlation effects and is a challenging problem.[51,52]

There is also a restriction for weak coupling. If the coupling parameter is too low, the cluster radius is no longer well defined, and the density becomes very inhomogeneous. The analytical model, however, is based on a homogeneous density profile. While it would be possible to use more realistic density profiles in the Navier-Stokes equation, e.g., from simulations, this would complicate the analysis and make it more difficult to compare with the results for a uniform system. Moreover, the viscosity coefficient in Eq. (4) is constant, i.e., we assign a single (density independent) viscosity to the cluster. Considering also the restrictions at strong coupling, this leads us to the conclusion that the method is best applied for intermediate values of the coupling parameter.

It was shown that 2D Yukawa plasmas exhibit shear thinning,[20] i.e., a decrease of the viscosity at high shear rates. We investigated the dependence of the measured viscosity on the shear rate for $r_0/\lambda = 2$ and $\tilde{T} = 0.2$. Varying the amplitude in the range $A = 0.4\ldots0.85$ revealed no systematic influence on the results. In addition, the angular velocities are well below the trap frequency ω_0, see Fig. 4. We may thus conclude that the applied shear rates are sufficiently low to minimize effects related to shear thinning.

V. CONCLUSION

In summary, we have presented a method to determine the viscosity of confined, two-dimensional dust clusters. An external force applied to the outer part of the cluster creates a sheared velocity profile, which is determined by angular momentum transfer to the inner parts through viscosity and removal of angular momentum through friction with the neutral gas. The viscosity can be measured by comparing the velocity profile with a solution of the Navier-Stokes equation. We performed molecular dynamics simulations to demonstrate the feasibility of the method and found good agreement of our results with previous simulations for macroscopic 2D Yukawa plasmas.[19,20] The simulated setup could be directly realized experimentally with several laser beams that act on the outer part of the cluster.[31]

ACKNOWLEDGMENTS

This work was supported by the DFG via SFB-TR24, projects A7 and A9.

[1]G. E. Morfill and A. V. Ivlev, "Complex plasmas: An interdisciplinary research field," Rev. Mod. Phys. **81**, 1353 (2009).
[2]M. Bonitz, C. Henning, and D. Block, "Complex plasmas: A laboratory for strong correlations," Rep. Prog. Phys. **73**, 066501 (2010).
[3]P. Hartmann, A. Douglass, J. C. Reyes, L. S. Matthews, T. W. Hyde, A. Kovács, and Z. Donkó, "Crystallization dynamics of a single layer complex plasma," Phys. Rev. Lett. **105**, 115004 (2010).
[4]A. Schella, M. Mulsow, A. Melzer, H. Kählert, D. Block, P. Ludwig, and M. Bonitz, "Crystal and fluid modes in three-dimensional finite dust clouds," New J. Phys. **15**, 113021 (2013).
[5]A. Schella, M. Mulsow, A. Melzer, J. Schablinski, and D. Block, "From transport to disorder: Thermodynamic properties of finite dust clouds," Phys. Rev. E **87**, 063102 (2013).
[6]B. Liu, J. Goree, and Y. Feng, "Non-Gaussian statistics and superdiffusion in a driven-dissipative dusty plasma," Phys. Rev. E **78**, 046403 (2008).
[7]V. Nosenko, S. Zhdanov, A. V. Ivlev, G. Morfill, J. Goree, and A. Piel, "Heat transport in a two-dimensional complex (dusty) plasma at melting conditions," Phys. Rev. Lett. **100**, 025003 (2008).
[8]V. Nosenko, J. Goree, and A. Piel, "Cutoff wave number for shear waves in a two-dimensional Yukawa system (dusty plasma)," Phys. Rev. Lett. **97**, 115001 (2006).
[9]P. Ludwig, W. J. Miloch, H. Kählert, and M. Bonitz, "On the wake structure in streaming complex plasmas," New J. Phys. **14**, 053016 (2012).
[10]A. Ivlev, H. Löwen, G. Morfill, and C. P. Royall, *Complex Plasmas and Colloidal Dispersions: Particle-Resolved Studies of Classical Liquids and Solids* (World Scientific, Singapore, 2012).

[11]Z. Donkó, G. J. Kalman, and P. Hartmann, "Dynamical correlations and collective excitations of Yukawa liquids," J. Phys.: Condens. Matter **20**, 413101 (2008).
[12]Z. Donkó, J. Goree, P. Hartmann, and B. Liu, "Time-correlation functions and transport coefficients of two-dimensional Yukawa liquids," Phys. Rev. E **79**, 026401 (2009).
[13]T. Ott and M. Bonitz, "Is diffusion anomalous in two-dimensional Yukawa liquids?" Phys. Rev. Lett. **103**, 195001 (2009).
[14]G. Kudelis, H. Thomsen, and M. Bonitz, "Heat transport in confined strongly coupled two-dimensional dust clusters," Phys. Plasmas **20**, 073701 (2013).
[15]T. Ott, M. Bonitz, and Z. Donkó, "The effect of correlations on the heat transport in a magnetized plasma," e-print arXiv:1506.03605.
[16]K. Y. Sanbonmatsu and M. S. Murillo, "Shear viscosity of strongly coupled Yukawa systems on finite length scales," Phys. Rev. Lett. **86**, 1215 (2001).
[17]T. Saigo and S. Hamaguchi, "Shear viscosity of strongly coupled Yukawa systems," Phys. Plasmas **9**, 1210 (2002).
[18]G. Salin and J.-M. Caillol, "Transport coefficients of the Yukawa one-component plasma," Phys. Rev. Lett. **88**, 065002 (2002).
[19]B. Liu and J. Goree, "Shear viscosity of two-dimensional Yukawa systems in the liquid state," Phys. Rev. Lett. **94**, 185002 (2005).
[20]Z. Donkó, J. Goree, P. Hartmann, and K. Kutasi, "Shear viscosity and shear thinning in two-dimensional Yukawa liquids," Phys. Rev. Lett. **96**, 145003 (2006).
[21]Z. Donkó and P. Hartmann, "Shear viscosity of strongly coupled Yukawa liquids," Phys. Rev. E **78**, 026408 (2008).
[22]P. Hartmann, M. C. Sándor, A. Kovács, and Z. Donkó, "Static and dynamic shear viscosity of a single-layer complex plasma," Phys. Rev. E **84**, 016404 (2011).
[23]Y. Feng, J. Goree, and B. Liu, "Frequency-dependent shear viscosity of a liquid two-dimensional dusty plasma," Phys. Rev. E **85**, 066402 (2012).
[24]A. Budea, A. Derzsi, P. Hartmann, and Z. Donkó, "Shear viscosity of liquid-phase Yukawa plasmas from molecular dynamics simulations on graphics processing units," Contrib. Plasma Phys. **52**, 194 (2012).
[25]A. Z. Kovács, P. Hartmann, and Z. Donkó, "Dynamic shear viscosity in a 2d Yukawa system," Contrib. Plasma Phys. **52**, 199 (2012).
[26]Z. Donkó, P. Hartmann, and J. Goree, "Shear viscosity of strongly-coupled two-dimensional Yukawa liquids: Experiment and modeling," Mod. Phys. Lett. B **21**, 1357 (2007).
[27]V. Nosenko and J. Goree, "Shear flows and shear viscosity in a two-dimensional Yukawa system (dusty plasma)," Phys. Rev. Lett. **93**, 155004 (2004).
[28]A. Gavrikov, I. Shakhova, A. Ivanov, O. Petrov, N. Vorona, and V. Fortov, "Experimental study of laminar flow in dusty plasma liquid," Phys. Lett. A **336**, 378 (2005).
[29]O. Vaulina, O. Petrov, A. Gavrikov, X. Adamovich, and V. Fortov, "Experimental study of transport of macroparticles in plasma rf-discharge," Phys. Lett. A **372**, 1096 (2008).
[30]V. E. Fortov, O. F. Petrov, O. S. Vaulina, and R. A. Timirkhanov, "Viscosity of a strongly coupled dust component in a weakly ionized plasma," Phys. Rev. Lett. **109**, 055002 (2012).
[31]J. Schablinski, D. Block, A. Piel, A. Melzer, H. Thomsen, H. Kählert, and M. Bonitz, "Laser heating of finite two-dimensional dust clusters: A. Experiments," Phys. Plasmas **19**, 013705 (2012).
[32]H. Thomsen, H. Kählert, M. Bonitz, J. Schablinski, D. Block, A. Piel, and A. Melzer, "Laser heating of finite two-dimensional dust clusters: B. Simulations," Phys. Plasmas **19**, 023701 (2012).
[33]J. Schablinski, D. Block, J. Carstensen, F. Greiner, and A. Piel, "Sheared and unsheared rotation of driven dust clusters," Phys. Plasmas **21**, 073701 (2014).
[34]H. Thomsen, P. Ludwig, M. Bonitz, J. Schablinski, D. Block, A. Schella, and A. Melzer, "Controlling strongly correlated dust clusters with lasers," J. Phys. D: Appl. Phys. **47**, 383001 (2014).
[35]H. Kählert, J. Carstensen, M. Bonitz, H. Löwen, F. Greiner, and A. Piel, "Magnetizing a complex plasma without a magnetic field," Phys. Rev. Lett. **109**, 155003 (2012).
[36]R. Mannella, "Quasisymplectic integrators for stochastic differential equations," Phys. Rev. E **69**, 041107 (2004).
[37]*Handbook of Mathematical Functions With Formulas, Graphs, and Mathematical Tables*, edited by M. Abramowitz and I. A. Stegun (National Bureau of Standards, Washington, D.C., 1972), 10th printing.
[38]P. S. Epstein, "On the resistance experienced by spheres in their motion through gases," Phys. Rev. **23**, 710 (1924).
[39]J. Carstensen, H. Jung, F. Greiner, and A. Piel, "Mass changes of microparticles in a plasma observed by a phase-resolved resonance method," Phys. Plasmas **18**, 033701 (2011).
[40]J. Carstensen, F. Haase, H. Jung, B. Tadsen, S. Groth, F. Greiner, and A. Piel, "Probing the plasma sheath by the continuous mass loss of microparticles," IEEE Trans. Plasma Sci. **41**, 764 (2013).
[41]J. Wrighton, J. W. Dufty, H. Kählert, and M. Bonitz, "Theoretical description of Coulomb balls: Fluid phase," Phys. Rev. E **80**, 066405 (2009).
[42]J. Wrighton, J. W. Dufty, M. Bonitz, and H. Kählert, "Shell structure of confined charges at strong coupling," Contrib. Plasma Phys. **50**, 26 (2010).
[43]Y. Feng, J. Goree, and B. Liu, "Observation of temperature peaks due to strong viscous heating in a dusty plasma flow," Phys. Rev. Lett. **109**, 185002 (2012).
[44]T. Ott, M. Stanley, and M. Bonitz, "Non-invasive determination of the parameters of strongly coupled 2d Yukawa liquids," Phys. Plasmas **18**, 063701 (2011).
[45]The approximate error for κ and Γ in our simulations is on the order of 5%.
[46]T. S. Ramazanov and K. N. Dzhumagulova, "Shear viscosity of dusty plasma obtained on the basis of the Langevin dynamics," Contrib. Plasma Phys. **48**, 357 (2008).
[47]Z. Donkó, J. Goree, and P. Hartmann, "Viscoelastic response of Yukawa liquids," Phys. Rev. E **81**, 056404 (2010).
[48]Y. Feng, J. Goree, and B. Liu, "Viscoelasticity of 2d liquids quantified in a dusty plasma experiment," Phys. Rev. Lett. **105**, 025002 (2010).
[49]Y. Feng, J. Goree, and B. Liu, "Viscosity calculated in simulations of strongly coupled dusty plasmas with gas friction," Phys. Plasmas **18**, 057301 (2011).
[50]H. Thomsen and M. Bonitz, "Resolving structural transitions in spherical dust clusters," Phys. Rev. E **91**, 043104 (2015).
[51]H. Bruhn, H. Kählert, T. Ott, M. Bonitz, J. Wrighton, and J. W. Dufty, "Theoretical description of spherically confined, strongly correlated Yukawa plasmas," Phys. Rev. E **84**, 046407 (2011).
[52]F. Gu, H.-J. Wang, and J.-T. Li, "Density functional theory for the ground state of spherically confined dusty plasma," Phys. Rev. E **85**, 056402 (2012).